Egyptian Journal of Aquatic Biology & Fisheries
Zoology Department, Faculty of Science,
Ain Shams University, Cairo, Egypt.
ISSN 1110 – 6131
Vol. 28(5): 1733 – 1754 (2024)
www.ejabf.journals.ekb.eg

Comparative Studies on Antibacterial Potentials of Biosynthesized Cerium Oxide and Zinc Oxide Nanoparticles Against Fish Pathogens

Joseph Olugbojo[1*], Adeolu Akinyemi[2], Samuel Obasa[2] , Enock Dare
[1]Department of Biological Sciences, Bells University of Technology, Ota, Ogun State, Nigeria
[2]Department of Aquaculture and Fisheries Management, Federal University of Agriculture, Abeokuta, Ogun State, Nigeria
[3]Department of Chemistry, Federal University of Agriculture, Abeokuta, Ogun State, Nigeria

[*] **Corresponding Author: josephgbojo2012@gmail.com**

ARTICLE INFO
Article History:
Received: July 14, 2024
Accepted: Sept. 27, 2024
Online: Oct. 19, 2024

Keywords:
Nanoparticles,
Plant-mediated synthesis,
Scanning electron microscopy,
X-ray diffraction,
Fish pathogens

ABSTRACT
Plant-mediated synthesis of nanoparticles has gained significant attention due to its eco-friendliness, non-toxic nature, ease of preparation, and biocompatibility. Likewise, phytochemicals have been recognized as effective bio-reductants and capping agents in the formation of nanoparticles. The aim of this study was to compare the antibacterial potentials of biosynthesized cerium oxide and zinc oxide nanoparticles (CeO_2NPs and ZnONPs) against selected fish pathogens, *Aeromonas hydrophila*, *Aeromonas schubertii*, *Bacillus subtilis*, *Bacillus cereus*, and *Klebsiella pneumoniae*. Qualitative analysis of *Carica papaya* leaf extract was conducted to examine the biomolecules present, followed by the biosynthesis of the nanoparticles. The obtained CeO_2NPs and ZnONPs were characterized through UV-visible spectrophotometry, scanning electron microscopy, energy-dispersive X-ray spectroscopy, X-ray diffraction, and Fourier-transform infrared spectroscopy to confirm the formation of the nanoparticles. The results showed that CeO_2NPs had a spherical shape with an average size of 46.34nm, while ZnONPs exhibited a cylindrical shape with an average size of 43.77nm. Antibacterial sensitivity tests (AST) indicated that ZnONPs had greater antibacterial potential than CeO_2NPs against *A. hydrophila* (0.00 and 13.00 ± 1.15mm), *A. schubertii* (16.50 ± 1.73 and 15.50 ± 0.58mm), *B. cereus* (0.00 and 17.00 ± 1.15mm), and *K. pneumoniae* (13.00 ± 1.15 and 16.50 ± 0.58mm). However, CeO_2NPs were more effective against *B. subtilis* than ZnONPs (12.00 ± 1.15 and 13.00 ± 1.15mm). Both nanoparticles showed significant differences in their AST values against *A. hydrophila*, *B. cereus*, and *K. pneumoniae* ($P< 0.05$), while no significant difference was observed against *A. schubertii* and *B. subtilis*. Based on these findings, it can be concluded that ZnONPs are more effective than CeO_2NPs against *A. hydrophila*, *B. cereus*, and *K. pneumoniae*, and therefore may be useful in treating fish diseases caused by these pathogens.

INTRODUCTION

Fish living in their natural environment usually harbor bacterial pathogens. The breakage of the immunological barrier of fish due to the attack on fish muscles by pathogens is likely to occur when fish are cultured in environment with high

contamination of faecal coliforms **(Guzman *et al.*, 2004)**. Additionally, the use of antibiotics in treating ponds or fish has not achieved the desired outcome for optimum performance, instead, bacteria are becoming more resistant to them, coupled with the toxicity effect on water and aquatic lives. Hence, there is a need for alternative antibacterial agents, which should be eco-friendly, non-toxic and biocompatible. Nanomaterials have been found to play a very vital role in this regard, especially where antibiotics usually fail **(Pelgrift & Friedman, 2013)**. The use of nanomaterial will help to prevent the problem of toxicity threatening water and aquatic organism. It will also prevent bacteria from easily developing resistance due to the possibility of improving sizes, shapes, composition and crystallinity, which are the intrinsic properties that determine effectiveness of any nanoparticle (**Sharma *et al.*, 2009)**.

Nanotechnology can be defined as the synthesis, characterization, exploration and application of nano-sized (1-100nm) materials for the development of science. It deals with the materials whose structures exhibit significantly novel and improved physical, chemical, and biological properties, because of their ultra small size. Nanotechnology is also applicable in medicine, for diagnosis, therapeutic drug delivery, early disease detection and the development of treatments for many diseases and disorders. It is a highly promising technology which can be deployed to design and develop numerous types of novel products **(Huang *et al.*, 2009; Nikalje, 2015)**.

The development of nanoparticles (NPs) and nanostructures (NS) materials through exploration of biodiversity of plants to reduce metal ions has been adjudged as a widespread application in recent years. Phytochemicals present in plants have been reported as the source of reducing and capping activities, unlike the chemical method which involves the use of hash and toxic chemicals often absorbed in NP surfaces, and consequently renders chemically synthesize NPs, inadequate for medical applications **(Parashar & Srivastava, 2009)**.

In addition, plant biomolecules such as polyphenols, carbohydrates and essential oils are known to contain active functional groups, viz. aldehyde, amine, and carboxyl. These functional groups are the sources of reducing and capping potentials of plants for the development of NPs **(Harekrishna *et al.*, 2009)**.

Cerium oxide nanoparticle is a pale yellow powder, with the chemical formula CeO_2. It is very stable and biologically compatible. It has always been used to produce catalyst, therapeutic agents, antimicrobial and anti-nematodal agent, etc. Until recent time, CeO_2NP is usually synthesized through physical and chemical methods. This approach usually involves toxic reducing agents, which pose a serious threat to plants, animals and ecosystem in general. Moreover, the nanoparticles that were produced using such methods are usually not stable, very noxious and ineffective **(Parashar & Srivastava, 2009)**.

Different applications of green synthesized cerium oxide nanoparticles have been reported which include: antimicrobial, anticancer, larvicidal, photocatalyst, and antioxidant. However, antimicrobial application has been the most exploited among several other applications **(Maqbool *et al*., 2016; Elahi *et al*., 2018; Miri *et al*., 2019)**. Features, like high yield, long stability, and better morphology can be obtained through green synthesis approach, especially from the plant source **(He *et al*., 2015)**.

Biogenic synthesis of ZnONPs has only been reported in few journals. Due to lesser research work on ZnONPs nanoparticles, there are limited data on their diverse biological properties. Generally, plant-mediated synthesis of zinc oxide nanoparticles is a rapid, eco-friendly, and less or non-toxic approach, especially when the agent of green synthesis is plant extracts **(Noorjahan, 2019)**.

Among metal oxide nanoparticles, zinc oxide nanoparticle (ZnONPs) is another promising inorganic material NPs with multifaceted benefits. The excellent optical, semiconducting, and photoelectric properties make ZnONPs exploited across various industries such as composites, cosmetics, catalysis, energy storage, electronics, textile, and health **(Kumar *et al*., 2014)**. Apart from being non-toxic, they are also biocompatible, cheaper, and has various biomedical applications such as antibacterial and antiparasitic agent, among others **(Alyamani, *et al*., 2021)**.

Initially, ZnONPs were commonly synthesized through physical and chemical means, just like CeO_2NPs. The physical methods of synthesis are accompanied with high-energy requirements, while chemical synthesis involves the use of noxious chemicals, making both methods non environment-friendly, expensive, and laborious **(Diallo *et al*., 2015)**, thus paving a way for green synthesis.

In this research, a rapid synthesis of both CeO_2NP and ZnONPs via a complete environmental friendly procedure was reported using aqueous leaf extracts of *Carica papaya* as a good reducing and stabilizing agent.

Carica papaya (Pawpaw – common name) was chosen due its excellent therapeutic activities, especially as antibacterial which has been used on many occasions to treat fish diseases **(Rahmani & Aldebasi, 2016; Singh *et al*., 2019; Husain *et al*., 2023; Muahiddah & Diamahesa, 2023)**. Several studies on bioactive component of different parts of *C. papaya* revealed that they contain phytochemicals such as: alkaloids, saponins, tannins, flavonoids and glycosides among others, and have been used as antibacterial, anti-inflammatory, antiviral, hypoglycemic, antitumor and several other therapeutic and prophylactic applications **(Natarajan & Vidhya, 2016)**.

Therefore, due to its ease of availability and medicinal importance, *Carica papaya* (Leaf) was chosen for biosynthesis of CeO_2NP and ZnONPs. Use of common reducing agent helps easy comparison in order to arrive at a justifiable result. Easy accessibility of

C. papaya will also assist in a large scale production toward a wide range of therapeutic and prophylactic usage **(Paul *et al.*, 2013; Nagarathan *et al*., 2021)**.

The main objective of this research was to compare the antibacterial potentials of cerium oxide nanoparticles, and zinc oxide nanoparticles on some common bacteria fish pathogens, for onward recommendation to the fish farmers for improving fish production, food security, and help to alleviate poverty, especially among the rural dwellers in Nigeria, as a contribution toward the United Nations sustainable development goals (SDG 1 and 2).

MATERIALS AND METHODS

1. Preparation of *Carica papaya* leaf extract

The leaves of *Carica papaya* (pawpaw) were collected at Bells University of Technology campus, Ota, Ogun State. They were washed, and air-dried for about two weeks. The dried *C. papaya* leaves were cut into small pieces. 10g of leaves were weighed, washed, using deionized water, and boiled with 100ml of deionized water at 70˚C for 1h. After boiling, the leaf extract was separated by filtration (using Whatman No.1 filter paper) and kept in the fridge at 5^0C for further use **(Singh *et al*., 2019)**.

2. Phytochemical screening of *Carica papaya* leaf extract

Phytochemical analysis of *Carica papaya* leaf extract (CPLE) was analyzed using standard approach **(Ali *et al,* 2018; Ghotekar, 2019)**. This includes: phenols, alkanoids, saponins, steroids, flavonoids, glycosides, terpenoids, proteins, and carbohydrates.

2.1. Saponins

Equal volume (2ml) of distilled water was added to an equal volume (2 ml) of plant extract. It was mixed and vigorously shaken in a graduated cylinder. A layer of 1cm thick foam confirmed the presence of saponins.

2.2. Flavonoids

10 drops of dilute hydrochloric acid was mixed with 0.5ml of plant extract in a test tube, and then a small quantity of magnesium were added. Formation of pink, red or brown colour depicted the presence of flavonoids.

2.3. Phenols (Ellagic acid test)

5% of glacial acetic acid was added to 1ml of plant extract in drops, then few drops of 5% $NaNO_2$ solution were added. The formation of muddy brown color showed that phenol is present in the sample.

2.4. Betacyanins

One ml of 2N Sodium hydroxide was added to 2ml of leaf extract and heated at 100°C for about 5min to determine if betacyanin is present. The formation of yellow color depicted the presence of betacyanin in the plant extract.

2.5. Coumarins

Equal volume (1ml) of 10% NAOH solution was added to an equal volume (1ml) of the plant extract. Yellow color formation confirmed the existence of coumarins in the test samples

2.6. Tannins ($FeCl_3$ test)

5% $FeCl_3$ was added to the plant extract in a ratio of 2 to 1. The presence of Tannin was confirmed with the immediate appearance of greenish black or dark blue color

2.7. Steroids

2 ml of both plant extract and chloroform (1ml from each) were added together. Then, a few drops of conc. H_2SO_4, was added; this led to brown ring formation. The appearance of this ring marked the existence of steroids. However, the appearance of bluish-brown ring color marked the presence of phytosteroids in the test samples.

2.8. Carbohydrates

2 milliliters of test solution and Benedict's solution (in drops) were mixed together, and then boiled in water bath of over a bunsen burner flame. The presence of carbohydrates in the test samples was confirmed by the formation of reddish brown precipitate.

2.9. Glycosides

Glacial acetic (1ml) acid and plant extract (1ml) were added together, and allowed to cool. After cooling, 2 drops of $FeCl_3$ were added, and equal drops (2 drops) of concentrated H_2SO_4 were also added along the walls of the test tube. Reddish brown color ring formed at the junction of two layers showed the presence of glycosides.

2.10. Terpenoids

1% HCl was added to the plant extract in a ratio of 1 to 2, and left for 5-6 hrs. in the same condition. After about 6 hours, 1ml of Trim-Hill reagent was added and heated in a boiling water bath for 5-10min. The presence of terpenoids was confirmed by bluish green color.

2.11. Alkaloids (Wagner's test)

2ml of extract was first acidified with 1.5% v/v of hydrochloric acid. Then, a few Wagner's reagent was added in drops. The formation of a yellow or brown precipitate depicted the presence of Alkanoid in the plant extract.

2.12. Betacyanins

To the plant extract, some drops of NAOH were added, the conversion of the extract to a dull yellow color showed the presence of betacyanin in the sample. İn reverse, a few drops of HCL (Conc.) were added, the disappearance of the color showed that betacyanin was present in the sample.

3. Synthesis of cerium oxide nanoparticles

One millimolar (mM) of Cerium (III) chloride heptahydrate ($CeCl_3$.$7H_2O$) obtained from Sigma-Aldrich company, U.K. was prepared as a standard solution by dissolving 0.0932g in 250ml of deionized water in a standard flask. The mixture was stirred using a magnetic stirrer at a room temperature until a homogeneous solution was formed. 100ml was taken into another conical flask and 10ml of *Carica papaya* leaf extract was added. The reaction mixture was kept under continuous stirring with magnetic stirrer, and heated on a hot plate at 60℃ for about 2hrs. **(Renganathan *et al.*, 2018)**. Cerium oxide nanoparticles were collected as precipitate at the base of the conical flask. It was decanted and centrifuged at 4000rpm for 30 minutes. It was further dried in hot air oven at 60℃ overnight. The obtained pellets (Cerium oxide Nanoparticles, CeO_2NPs) were calcinated at 400℃ in a muffle furnace for 4-6 hours to obtain a purer product. The pure cerium oxide nanoparticles were kept for characterization.

4. Synthesis of zinc oxide nanoparticles

Green synthesis of zinc oxide nanoparticles was carried out through a well improved procedure, taking a cue from the previous methods **(Arumugam *et al*, 2015; Rani *et al*, 2020)**, with modifications. 2.975g of zinc nitrate hexahydrate obtained from Qualikems Fine Chemical Pvt. Limited, India was weighed in a clean conical flask, and 80ml of distilled water was added. Using magnetic stirrer, the solution was stirred till a homogenous solution was attained. It was then transferred into a 100ml standard flask and make up to the mark with 20ml to make 100ml standard solution at 100 millimolar (100mM). In addition, 1Molar NAOH was prepared by dissolving 4g of NaOH in 100ml of distilled water as a standard solution. Initial 100mM of zinc nitrate solution ($Zn(NO3)2.6H_2O$) was transferred into a clean 250ml conical flask and kept under stirring in a hot plate with magnetic stirrer at 60℃. To this, 15ml of *Carica papaya* leaf extract was added in drops until there was a change in color to golden yellow. The pH of the reaction mixture was checked, and adjusted to 12 by addition of 1M NaOH. A white cloudy appearance marks the formation of ZnO nanoparticles. This was allowed to stand in the same condition for about 2hrs (for the reaction to complete and to fully precipitate the ZnONPs formed). It was further incubated overnight at room temperature. It was then decanted and the suspension was centrifuged at 4000rpm for 30 minutes. The wet pellet was poured into a clean petri dish, and heated in a hot air oven at 150℃ till about 6 hours. The dried pellet obtained was ground into powder, and kept for characterization

5. Characterization techniques

UV-Vis spectrophotometer (BOSCH 750N) was used to analyze the optical characteristics of the nanoparticles at 200-800nm wavelength.

Surface morphology and microstructure of the samples were determined using the field emission scanning electron microscope, GEMINI Ultra 55 (FESEM). The samples were fixed on carbon tape and kept for overnight drying. The samples were gold coated (100nm) and viewed under the scanning electron microscope (at 5kv), which has an energy dispersive x-ray analysis unit (EDX).

Analysis of the X-ray Diffraction pattern to determine the crystallinity of the CeO_2NPs, and ZnONPs was carried out using a Bruker AXS D8 Diffractometer, equipped with nickel filtered Cu Ka radiation (k = 1.5418 Å) at 40kV and 40mA at room temperature.

Chemical properties, effect of biomolecules, and the type of bonds present were determined using Perkin-Elmer 100 series Fourier transform Infra-red spectrophotometer (FT-IR), which functioned at $4ms^{-1}$ scan rate over the range of $4000\text{-}650cm^{-1}$ wavenumber in the diffuse reflectance mode at a resolution of $6cm^{-1}$ in KBr pellets.

6. *in-vitro* Antibacterial activity of CeO_2NP and ZnONP

Antibacterial potential of the nanoparticles was screened using agar well diffusion technique against bacterial pathogens. Sterile Mueller Hinton agar plates was swabbed using sterile L-shaped glass spreader with 18-24 hours old broth cultures *of Aeromonas hydrophila, Aeromonas Schubertii, Bacillus subtilis, Bacillus cereus and Klebsiella pneumonia* which were isolated from skin, gill, and gut of *Clarias gariepinus* (African mud catfish*),* and have been identified through morphological, biochemical and molecular characterization. Plates were then incubated for 24 hours. Using a sterile cork borer, wells of appropriate dimension were bored on each Petri dish. 200mg/ ml of each of the NPs (CeO_2NPs and ZnONPs) in sterile DMSO was used, while 200mg/ ml of antibacterial drug (Ofloxacin) dissolved in sterile DMSO was also used as control. 200mg/ ml was chosen after several trials with lesser concentrations did not yield good result. All plates were incubated at the same time at 37°C for 24hrs. After the period of incubation, the diameter of the zones of inhibition of each well was measured. Each sample (nanoparticles) was tested in two replicate, and the mean values were recorded. The MIC and MBC of each of the nanoparticles tested were also determined **(CLSI, 2012)**.

7. Statistical analysis

The numerical data obtained were analyzed using the one-way analysis of variance (ANOVA), SPSS 18 (Statistical Package for the Social Sciences) and 10

Microsoft Excel. Means were separated using Duncan multiple range test (DMRT) ($P \leq 0.05$).

RESULTS

1. Phytochemicals identified in *Carica papaya* leaf extract

The biomolecules present during the phytochemical screening carried out on *Carica papaya* leaf extract are shown in Table (1). They include flavonoids, alkaloid, tannins, phenols, and coumarins. These were responsible for the bio-reduction and capping during biosynthesis of the nanoparticles. Other listed phytochemicals were not found during the screening

Table 1. Phytochemicals identified in *Carica papaya* leaf extract

Serial number	Phytochemicals	*Carica papaya*
1	Saponin	**-**
2	Flavonoids	**+**
3	Alkanoids	**+**
4	Betacyanin	**+**
5	Phenol	**+**
6	Cumarins	**+**
7	Tannins	**-**
8	Steroids	**-**
9	Carbohydrates	**-**
10	Glycosides	**-**
11	Terpenoids	**-**

2. UV-Visible spectrophotometry (UV-Vis Spec) of CeO_2NPs and ZnONPs

The UV - Vis spectra of synthesized CeO_2NPs and ZnONPs as determined through UV-Visible spectrophotometer are shown in Fig. (1). CeO_2NPs were formed through a color change from yellow to brown, and display an optical absorption peak at 360 and 380nm in the UV region (Fig. 1a). ZnONPs were also formed through color change, from light brown to golden yellow, and then to a white cloudy appearance. It also display various absorption peaks at 320, 340, and 380nm in the UV region (Fig. 1b).

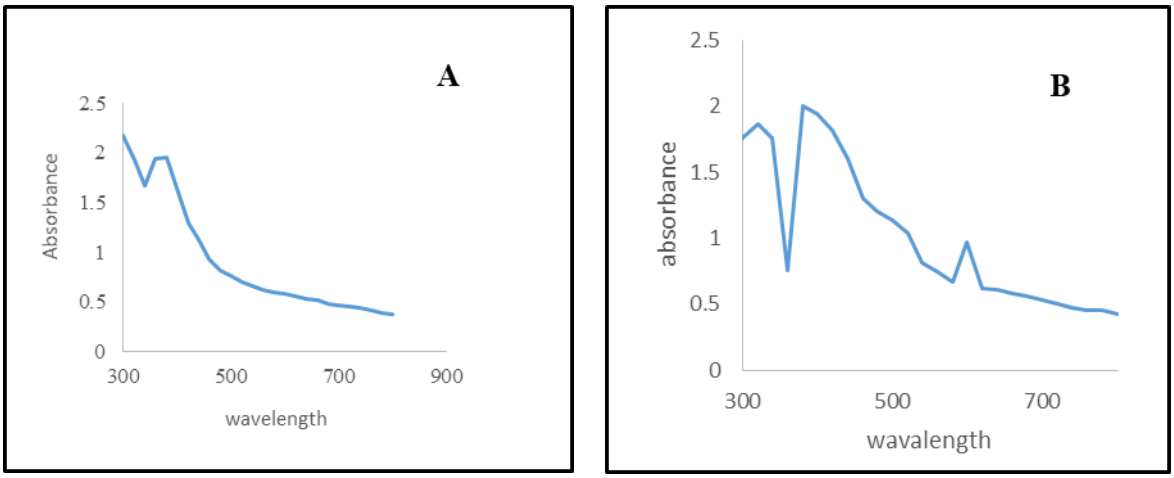

Fig. 1. (A) UV-visible spectrum of cerium oxide nanoparticles showing maximum absorption peak at 360 and 380nm. (**B**) UV-visible spectrum of zinc oxide nanoparticles showing maximum absorption peak at 240, 260, and 300nm

3. Functional group and bond characteristics of CeO_2NPs and ZnONPs

The spectroscopic analysis using FTIR was carried out in the range of 500-4000cm^{-1}. For cerium oxide nanoparticles (Fig. 2a), the FITR absorption peak was found between 989.11 and 3359.35cm^{-1} in the functional group and finger print region. Four important peaks could be found which are located at 3359.35, 2974.66, 1635.12, and 1380.70cm^{-1}. 3359.35cm^{-1} is a broad peak which corresponds to O-H stretching of phenol and alcohol group (usually stretches between 3200-3400 in the infrared region of the IR spectrum), 2974.66cm^{-1} corresponds to C-H stretching vibration of the alkane group, 1635.12cm^{-1} corresponds to C=O stretching of the carbonyl group which usually ranges between 1640-1680 within the infrared region of the IR spectrum, while 1380.70cm^{-1} is assigned to C-O stretching vibration of the phenolic compound and polysaccharide which provide stability due to successful capping of CeO_2NPs. For zinc oxide nanoparticles, six important peaks were also observed between 1098.62 and 3468.12cm^{-1} in the FTIR spectrum (Fig. 2b). They included: 3468.12, 2958.79, 1614.06, 1529.55, 1438.57, and 1098.62cm^{-1}. 3468.12cm^{-1} (broad peak) corresponds to the stretching vibration of the phenol group (O-H), which helped in bio-reduction, while the peak at 2958.79 is attributed to C-H stretching frequency of the alkane group (alkyl sp3 C-H). 1614.06 is assigned to C=O stretching frequency, arising from the interaction with the carbonyl and some aromatic group present in the extract. 1529.55cm^{-1} also corresponds to the amine bond (N=H), which is typical of the protein from the extract used in the biosynthesis. 1098.62cm^{-1} is assigned to the stretching vibration of C-O-C asymmetric band of ether at the finger print region which binds to the nanoparticle to ensure stability.

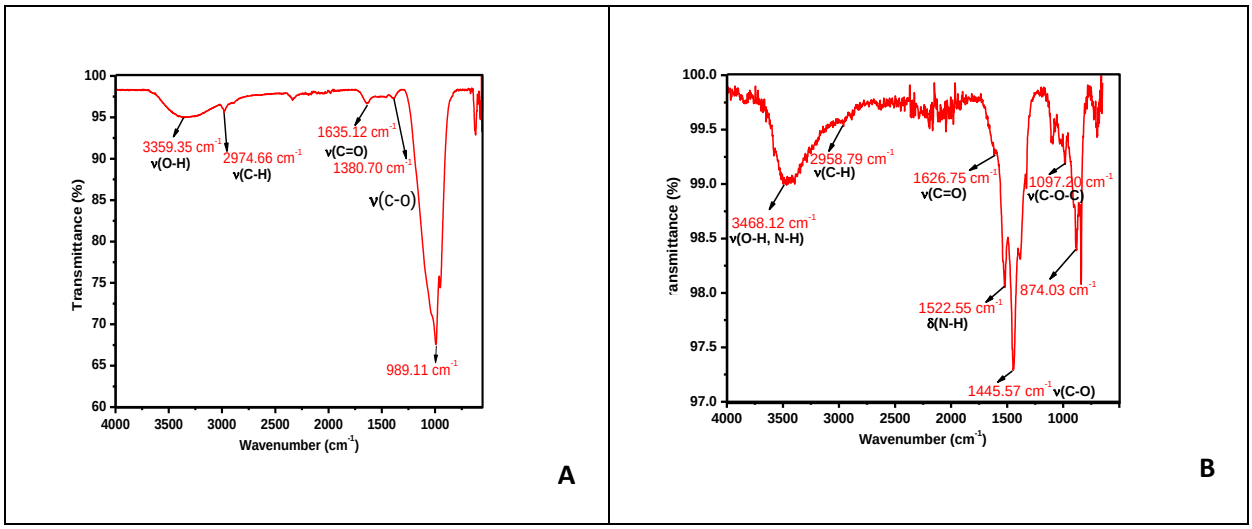

Fig. 2. (**A**) FTIR spectrum of the biosynthesized Cerium oxide nanoparticles. (**B**) FTIR spectrum of the biosynthesized zinc oxide nanoparticles. Both show bonds related to the biomolecules present in *Carica papaya* leaf extract

4. Diffraction patterns of CeO_2.NPs and ZnONPs

The XRD was used to determine the crystallinity and phase purity of the nanoparticles as observed in the diffractogram shown in Fig. (3). The diffraction patterns of cerium oxide nanoparticles (Fig. 3a) were observed at 2θ values. It shows four major peaks at various diffraction angles such as: 29.00, 33.46, 47.87 and 56.67^0, which also correspond to 111, 200, 220, and 311 reflection planes of CeO_2.NP, respectively. The XRD spectrum of zinc oxide nanoparticles were also observed at 2θ angular value (Fig. 3b). The diffraction pattern showed various diffraction peaks at 32.31, 34.87, 36.61, 48.00, 57.05, 63.16, and 68.40^0, which are in good accent with 100, 002, 101, 102, 110, 103, and 112 reflection planes

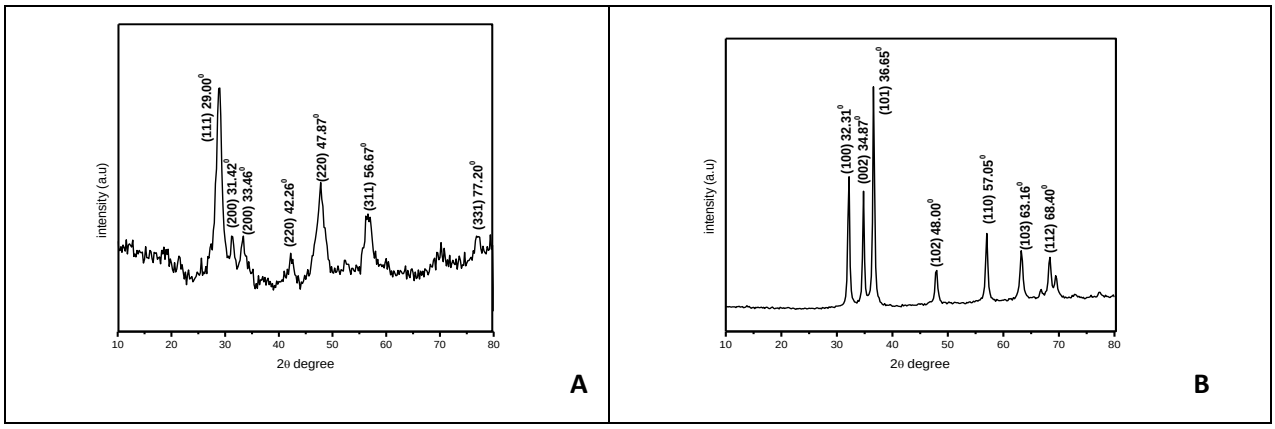

Fig. 3. (**A**) XRD pattern of cerium oxide nanoparticles showing different diffraction peaks at 2θ values. (**B**) XRD pattern of Zinc oxide nanoparticles showing different diffraction peaks at 2θ values

5. Particle size distribution, dimension and elemental compositions of CeO_2NPs and ZnONPs

SEM morphology of cerium oxide nanoparticles using field emission scanning electron microscopy (FESEM) are depicted in the photomicrograph (Fig. 4 a). The image revealed spherical shaped nanoparticles with an average particle size of 46.34nm. The particles were shown to be well distributed over the surface of the carbon coated SEM grid. EDX analysis (Fig. 4a) also revealed that cerium, oxygen and carbon were present. For zinc oxide nanoparticles, the surface morphology revealed cylindrical and spherical shaped nanoparticles, which are well distributed on the surface of the carbon coated SEM grid, with an average size of 43.77nm (Fig. 4b). This shows that the nanoparticles were well formed, and thus grew into single and separate particles. It revealed the ability of the phytochemicals to cap and stabilize the formed particles. The elemental composition from the EDX spectrum (Fig. 4b) shows that zinc, oxygen and carbon are present in the nanoparticles, while carbon and oxygen are carboxyl group from the plant chemicals used in the biosynthesis.

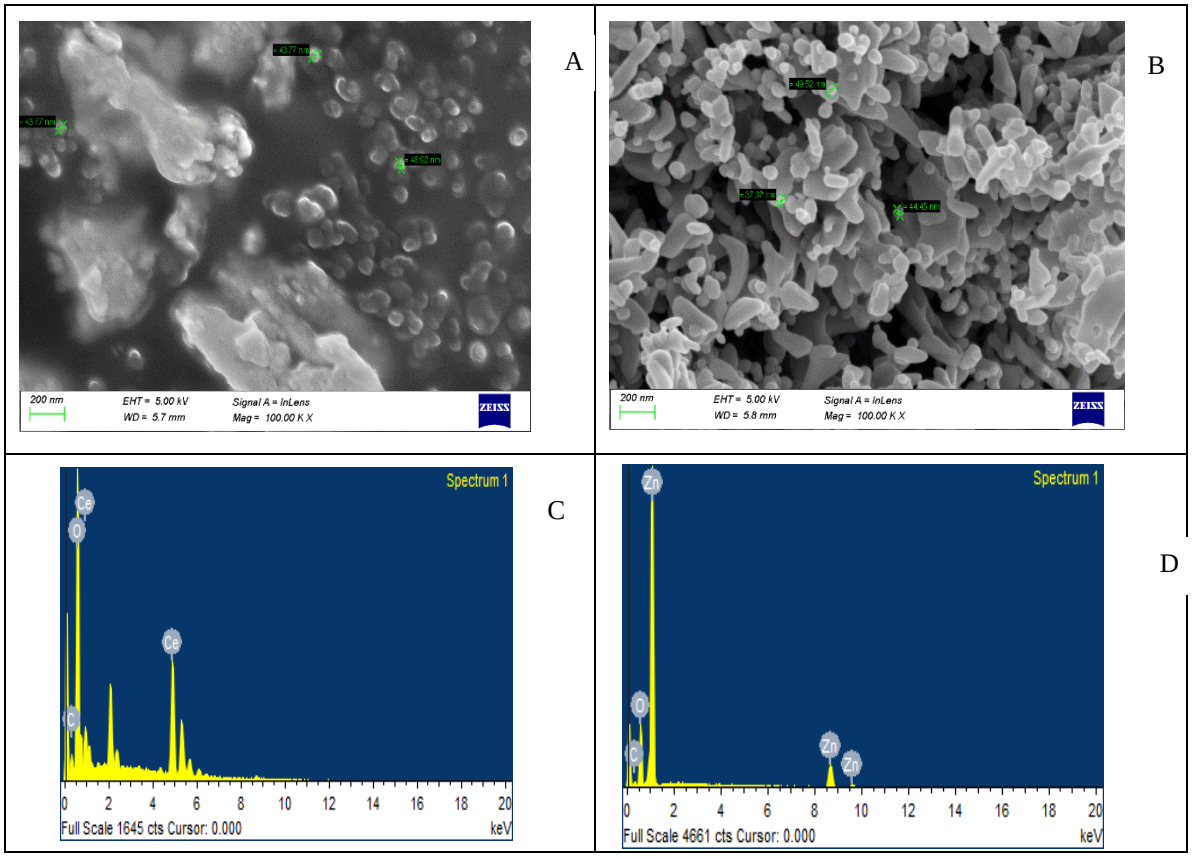

Fig. 4. (**A**) Surface morphology of CeO_2.NP NPs. (**B**) Surface morphology of ZnONPs NPs. (**C**) EDX spectrum of cerium oxide NPs. (**D**) EDX spectrum of zinc oxide NPs

6. Antibacterial activity of CeO_2.NPs and ZnONPs

The results of antibacterial activity of the biosynthesized CeO_2.NP and ZnONP using agar well diffusion method are shown in Table (2). The results showed zones of inhibition which are measured in millimeters. Only *A. schubertii* depicted higher inhibition zones with CeO_2NPs (16.50 ± 1.73^a) than ZnONPs (15.50 ± 0.58^a), whereas *A. hydrophila, B. subtilis, B. cereus,* and *K. pneumonia* showed higher inhibition zones when tested with ZnONPs (13.00 ± 1.15^b, 13.00 ± 1.15^a, 17.00 ± 1.15^b, and 16.50 ± 0.58^b) than CeO_2NPs (0.00, 12.00 ± 1.15^a, 0.00, 13.00 ± 1.15^a). Moreover, *A. hydrophila* and *B. cereus* were not sensitive to CeO_2NPs, showing no inhibition zone (0.00 ± 0.00^a) in each case at 200mg m^{-1} unlike ZnONPs, in which a highly significant ($P<0.05$) inhibition zone was depicted (13.00 ± 1.15^a and 17.00 ± 1.15^b, respectively). Nevertheless, the inhibition zones depicted by *A. schubertii* and *B. subtilis*, when tested with CeO_2NPs (16.50 ± 1.73^a, 12.00 ± 1.15^a), were not significantly different ($P> 0.05$) from those of ZnONPs (15.50 ± 0.58^a, 13.00 ± 1.15^a). The result obtained for ofloxacin (Control) showed the highest and highly significant ($P< 0.05$) inhibition zones on each bacterium (Table 2), which means that it is the most potent antibacterial among them all, except for its toxicity.

Table 2. Antibacterial sensitivity test of CeO_2NPs and ZnONPs nanoparticles (Mean ± SD in millimeters)

Antibacterial	*A. hydrophia*	*A. schebertii*	*B. subtilis*	*B. cereus*	*K. pneumoniae*
CeO2NPs	0.00 ± 0.00^a	16.50 ± 1.73^a	12.00 ± 1.15^a	0.00 ± 0.00^a	13.00 ± 1.15^a
ZnONPs	13.00 ± 1.15^b	15.50 ± 0.58^a	13.00 ± 1.15^a	17.00 ± 1.15^b	16.50 ± 0.58^b
Control (Ofloxacin)	26.50 ± 0.58^c	26.50 ± 0.58^b	25.50 ± 0.58^b	27.50 ± 0.58^c	26.50 ± 0.58^c

***Foot note:** Concentration- 200mg/ ml; Control- Ofloxacin; Mean ± SD with superscript of the same alphabet such as ‘a’,‘b’ or 'c' along the column shows no significant difference ($P>0.05$); Mean ±SD with a superscript of different alphabets such as ‘a’, ‘b' or 'c’, along the column shows that there was a significant difference ($P<0.05$)

7. Minimum inhibitory concentration of CeO2NPs and ZnONPs

The MIC results showed that ZnONPs have superior antibacterial efficacy compared to CeO_2NPs against *A. hydrophila* (0.00 and 25.52 ± 0.03mg/ mL), *B. subtilis* (100.00 ± 0.05mg/ mL), *B. cereus* (0.00 and 6.27 ± 0.02mg/ mL), and *K. pneumoniae* (50.10 ± 0.00 and 12.38 ± 0.14mg/ mL) (Table 3). The value of 0.00 for CeO_2NPs against *A. hydrophila* and *B. cereus* indicates no sensitivity or inhibition, even at 100mg/ mL. The results also showed that the MICs of both CeO_2NPs and ZnONPs for each pathogen are significantly different ($P< 0.05$).

Table 3. Minimum inhibitory concentration (MIC) of CeO_2.NPs and ZnONPs (Mean ± SD in mg/mL)

Antibacterial	*A. hydrophila*	*A. schubertii*	*B. subtilis*	*B. cereus*	*K. pneumonea*
CeO_2NPs	0.00±0.00[a]	12.52±0.02[a]	100.04±0.05[a]	0.00±0.00[a]	50.10±0.00[a]
ZnONPs	25.52±0.03[b]	12.53±0.03[b]	25.45±0.06[b]	6.27±0.02[b]	12.38±0.14[b]
Control (Ofloxacin)	3.13±0.01[c]	3.13±0.01[b]	4.67±1.17[c]	2.13±1.16[c]	3.13±0.01[c]

Foot note: Concentration- 100 mg/ml; Control- Ofloxacin; Mean ± SD with a superscript of the same alphabet such as 'a','b' or 'c' along the column shows no significant difference (P>0.05); Mean ±SD with a superscript of different alphabets such as 'a', 'b' or 'c', along the column shows that there was a significant difference (P<0.05).

8. Minimum bactericidal concentration (MBC) of CeO_2NPs and ZnONPs

Minimum bactericidal concentration (MBC) of CeO_2NPs and ZnONPs in Table (4) shows a more effective and highly potent ZnONPs. The results depicted the lowest lethal dose of each nanoparticle against the tested bacteria. ZnONPs required 25.02±0.02 mg mL^{-1} to kill *A. hydrophila*, while CeO_2NPs was not sensitive to *A. hydrophila*, even at 100mg mL^{-1}. On *A. schubertii*, there was no significant difference in their MBC (Table 4). Subsequently, at almost equal concentrations *(*12.53±0.03 and 12.59±0.01), CeO_2NPs and ZnONPs were able to destroy *A. schubertii*. ZnONPs also exhibited lower MBC (25.00±0.00) than CeO_2NPs (100.03±0.03) on *Bacillus subtilis*. Likewise on *K. pneumonia,* ZnONPs showed lower MBC (25.00±0.00) than CeO_2NP (50.01±0.01). *B. cereus* was not sensitive to CeO_2NPs, even at 100mg mL^{-1} (0.00) whereas ZnONPs was very effective against *K. pneimoniae*, even at the lower dose of 12.50±0.00mg mL^{-1}. The difference in the MBC displayed by each nanoparticle against each bacteria pathogen along the column is highly significant.

Table 4. Minimum bactericidal concentration (MBC) of CeO_2.NP and ZnONP nanoparticles (Mean ± SD in mg/mL)

Antibacterial	*Aeromonas hydrophila*	*Aeromonas schubertii*	*Bacillus subtilis*	*Bacillus cereus*	*Klebsiella pneumoniae*
CeO2NPs	0.00±0.00[a]	12.53±0.03[a]	100.03±0.03[a]	0.00±0.00[a]	50.01±0.01[a]
ZnONPs	25.02±0.02[b]	12.59±0.01[b]	25.00±0.00[b]	12.50±0.00[b]	25.00±0.00[b]
Control (Ofloxacin)	6.26±0.01[c]	6.26±0.01[c]	4.65±0.01[c]	6.27±0.01[c]	6.26±0.01[c]

Foot note: Concentration- 100 mg/ml; Control- Ofloxacin; Mean ± SD with a superscript of the same alphabet such as 'a','b' or 'c' along the column shows no significant difference (P>0.05); Mean ±SD with a superscript of different alphabets such as 'a', 'b' or 'c', along the column shows that there was a significant difference (P<0.05).

DISCUSSION

The current study involved biosynthesis, characterization and application of CeO_2NP and ZnONPs against some bacterial fish pathogens. Nanoparticles were characterized using spectroscopic and microscopic techniques. With UV-Vis spectroscopy, the absorption peak obtained at 360 and 380nm for CeO_2NP confirmed the typical absorption peaks for metallic ceria nanoclusters, which usually peak between 300-400nm, corresponding to the fluorite cubic structure of ceria; this is supported by previous studies **(Robinson *et al.*, 2009**; **Noorjahan, 2019)**. Likewise, the absorption peaks displayed by ZnONPs at 320, 340, and 380nm in the UV region falls within the typical absorption peak for metallic zinc oxide nanoparticles, usually found between 300-380nm **(Nagarathna *et al.*, 2021)**. In both cases, the onset of nucleation and growth started so rapidly and became steady till the reaction was completed. The color change during the reaction process was due to the excitation of electron and change in the electronic energy level of the metal oxide nanoparticles **(He & Lanhong, 2015)**. It also indicates the actual formation of the nanoparticles whose absorption peaks were formed at the UV region. The multiple absorption peaks at different wavelength by CeO_2NP and ZnONP show different shapes of the nanoparticles in each case **(Nateghi & Hajimirzababa, 2014)**.

The FTIR spectra of cerium oxide and zinc oxide nanoparticles were obtained in order to show the kind of bonds that were involved in the biogenic process. The obtained FTIR peaks for CeO_2NPs at various vibration modes and bond characteristics which depicted the presence of phenol, alcohol, alkane, and carbonyl groups are in agreement with previous studies **(Kumar *et al.*, 2014; Gnanasangeetha *et al.*, 2014; Timkur *et al.*, 2021)**. The participation of these biomolecules in the reduction and stabilization of CeO_2NP is clearly evident from the IR spectrum. This result was also supported by the previous works **(Nateghi & Hajimirzababa, 2014)** which described the participation of these phytochemicals in the redox process. Likewise, for zinc oxide nanoparticles, phenolic, carbonyl and alkane groups were implicated, in addition to amine and asymmetric bond of ether (observed at the finger print region of the IR spectrum) which bind to the nanoparticle to ensure stability. This showed that these nanoparticles are very rich in biomolecules such as polyphenols, alkaloids, flavonoids **(Diallo *et al.*, 2015; Alyamani *et al.*, 2021)**. From the previous studies **(Noorjahan, 2019)**, the stability of these synthesize nanoparticles (ZnONPs and CeO_2NPs) could presumably be accounted for the presence of free amino acids, and carboxylic acid group which have interacted with their surfaces by forming a wax covering them thereby preventing agglomeration. This result is also similar to the previous reports **(Gnanasangeetha *et al*, 2014; Alyamani *et al.*, 2021)** on the capping activities of plant biomolecules to ensure particle formation without agglomeration. Thus, the FTIR results confirmed that the phytochemicals found in the *Carica papaya* leaf extract, such as flavonoids, alkanoids,

phenols, betacyanin and coumarins (Table 1) were responsible for bio- reduction and stabilization reactions, which led to the formation of both CeO_2NPs and ZnONPs. It was also noted that some functional groups which correspond to certain compounds such as protein/amine group as mentioned above might not be captured during the phytochemical screening but were present, perhaps at minute quantity and could be identified during the IR analysis **(Gnanasangeetha *et al.*, 2014)**.

The diffraction pattern obtained at 2θ angular value for CeO_2NPs, as depictd in Fig. (3a) is in agreement with the result obtained by **Gnanasangeetha *et al*. (2014)** and **Rani (2020)**. The peaks matched well with those in the standard reference file (JCPDS No: 81-0792 - Joint committee on Powder Diffraction Standards) in both angular location and intensity. This confirmed the formation of spherical shape CeO_2NPs, as also indicated in SEM result in Fig. (4). No other peaks that depicted impurities were observed in the spectrum, and thus support the EDX result (Fig. 4c) **(Chenguo *et al.*, 2006)**.

The XRD analysis which was carried out to determine the crystallinity of the synthesized nanoparticle showed that both CeO_2NPs and ZnONP crystalline in nature. This result is in consonant with the previous studies **(Shen *et al*, 2018; Barzinjy, 2020)**. The peaks are relatively sharp, indicating the formation of the nano-crystalline phase which are indexed within the hexagonal zinc oxide wurtzite-type structure, in agreement with JCPDS card No. 36- 1451 **(Nateghi & Hajimirzababa, 2014; Shen *et al.*, 2018)**. Moreover, no other peaks showing impurities were observed in the spectrum. This confirms the formation of single ZnO phase as revealed in the EDX result in Fig. (4b). Moreover, the peak sharpness of CeO_2NP and ZnONPs indicates high crystallinity (Fig. 3) **(Balogun *et al*, 2021)**.

The surface microstructures of the CeO_2NPs, as represented by the SEM image, showed low degree of agglomeration, while ZnONPs did not show any form of agglomeration. Both nanoparticles were well spread on the carbon coated SEM grid to give them a large surface area to volume ratio, which is the typical characteristic of nanoparticles that determine their effectiveness as attested to by the previous work **(Noorjahan *et al*, 2019)**. Likewise, the particle sizes (46.34 and 43.77nm) obtained for CeO_2NPs and ZnONP, respectively, are in perfect agreement with the previous report (**Maqbool *et al.*, 2016; Jan *et al.*, 2020)**. **Noorjahan, 2019** also reported a cylindrical and spherical shaped zinc oxide nanocrystal on scanning electron microscope which was the same result obtained in this study. The high peak of Zn and Ce in the spectrum indicates high purity of the nanoparticles, as attested in the previous works **(Kwabena, 2019; Rani, 2020)**.

The overall results among the tested nanoparticles showed that, ZnONPs has excellent antibacterial potential than CeO_2NPs, and thus can be effectively used against *A. hydrophila, B. subtilis, B. cereus,* and *K. pneumonia* than CeO_2NPs. This result is supported by the previous finding in which *B. subtilis* and *K. pneumoniae* were found to

be highly susceptible to zinc oxide NPs. Their inhibition zones measured at 5mg/ mL was 9.5 ± 0.31 for *Bacillus subtilis* and 8.7 ± 0.18 for *K. pneumonia*. **(Jan *et al.*, 2020)**. Another finding revealed that ZnONPs exhibited a significant anti-*Bacillus subtilis* effect with 200µg ml^{-1} showing an optimum antibacterial activity between 1^{st} - 6^{th} hours of administration **(Uphadhyaya *et al.*, 2018; Djearamane *et al.*, 2023)**. It also reported a significant antibacterial activities of zinc oxide nanoparticles against *Aeromonas Veronii*, *Pseudomonas aeruginosa*, *Bacillus subtilis*, *Klebsiella. Pneumonia*, and *Staphilococcus aureus* infection. From the literature search, it was noted that, no report was found on *in-vitro* antibacterial sensitivity test of CeO_2NPs on *Aeromonas schubertii*. This shows that CeO_2NPs has not really been employed in the treatment of *A. schubertii* infection on fish. However, from this study the result showed that, cerium oxide can possibly perform better than zinc oxide nanoparticles against *A. schubertii*. Likewise, no work has so far been carried out on the pathogenic *B. cereus* both *in-vitro* and *in-vivo*. This could probably be that no infection has been reported yet. However, with the result obtained in this experiment there is a possibility of unrecorded occurrence of infection related to this.

Other studies revealed that zinc oxide nanoparticles exhibited an antibacterial activity through a damage to the cell membrane and entire cytoplasm, leading to bacterial cell death. In fish prophylaxis, zinc oxide nanoparticles have shown inhibitory effects against the growth of *A. hydrophila*. Likewise, it has been reported that the inclusion of ZnONPs in fish feed enhances immune response and exhibits high antibacterial activity and disease resistance against *A. hydrophila* **(Shaalan *et al.*, 2016; Jin & Jin, 2021; Harshitha *et al.*, 2023; Sherif *et al.*, 2023; Garani & Badsha, 2024)**.

While commonly used drugs may not be available sometimes due to high cost, high toxicity and challenge of bacteria resistance, ZnONPs or CeO^2NPs can be a cheaper and effective alternative against *A. Schubertii*. Besides, in view of the excellence performance of ZnONPs above CeO^2NPs, ZnONPs can be used to treat *A. hydrophila*, *B. cereus* and *klebsiella pneumonia* infections in fish. Since zinc oxide NPs is scarcely used unlike AgNp which has been widely explored, it can stand as a novel antibacterial agent, being cost- effective, and highly biocompatible, with an excellent result on fish health. It can be used to treat pond water before stocking, as well as serving as inclusion in fish diets for prophylactic and therapeutic applications.

The effectiveness of ZnONPs above CeO_2NP was found in the lesser quantity of ZnONPs that will be required to inhibit the growth of bacteria compared with CeO_2NPs in which more quantity will be required to inhibit bacteria growth. This result is supported by **Yass *et al.* (2023)** in which a lesser concentration of ZnONPs was used to inhibit the growth of a highly drug resistant *K. pneumonia* in an *in-vitro* experimental studies. This result corroborate with previous findings **(Sarkar *et al*, 2022; Yass *et al*, 2023)** on antibacterial potency of zinc oxide nanoparticles against fish pathogens.

CONCLUSION

Biosynthesis of CeO_2NPs and ZnONPs using *Carica papaya* leaf extract as bioreducing and capping agent were undertaken, and successfully confirmed through spectroscopic and microscopic characterization techniques.

The antibacterial sensitivity test results showed that zinc oxide nanoparticles (ZnONPs) were more effective against *A. hydrophila*, *Bacillus cereus*, and *K. pneumoniae* than cerium oxide nanoparticles (CeO_2NPs). In contrast, CeO_2NPs were more effective against *B. subtilis*. This trend was also observed in the minimum inhibitory concentration (MIC) and minimum bactericidal concentration (MBC) tests, which indicated that ZnONPs require a lower concentration to inhibit or kill the bacterial pathogens compared to CeO_2NPs.

These outcomes suggest that ZnONPs are more effective than CeO_2NPs in combating the tested fish pathogens. This confirms that ZnONPs can be effectively utilized for the treatment of fish ponds, fishing gear, and processing items that may become contaminated. Additionally, ZnONPs can be used for controlling and treating fish diseases and preventing zoonotic diseases.

It is important to note that *Carica papaya* was deliberately chosen for this study. While it is a common plant known for various therapeutic applications; its rich abundance of essential phytochemicals has yet to be fully explored. Often, *C. papaya* fruits are consumed merely as a food item, while other parts of the plant—such as the leaves, seeds, stems, roots, and flowers—are typically regarded as waste. We recommend further synthesis of nanoparticles using other parts of *C. papaya*.

This study represents the first report on the comparative antibacterial activity of *C. papaya* leaf extract-mediated synthesized cerium oxide and zinc oxide nanoparticles against pathogenic *A. hydrophila*, *A. schubertii*, *Bacillus subtilis*, *Bacillus cereus*, and *K. pneumoniae*.

ACKNOWLEDGEMENT:

The authors wish to appreciate Dr. Ayobami Ajisafe of Indian Institute of Science, Bangalore, India and Mr. Isaiah A.A of CEADESE Laboratory, Federal University of Agriculture, Abeokuta, for the characterization of the nanoparticles; Dr. S. Ejilude of Tuberculosis Reference Laboratory, University College Hospital, Ibadan, for his support during the sensitivity studies, and Dr. K.E Ogunsola, Bells University of Technology, Ota for proof-reading the manuscript.

CONFLICT OF INTEREST

The authors declare no conflict of interest on this research article.

REFERENCES

Ali, S.; Khan, M.R.; Sajid, I.M. and **Zahra, Z. (2018).** Phytochemical investigation and antimicrobial appraisal of *Parrotiopsis mjacquemontiana* (Decne). *Rehder BMC Complement Altern. Med.*, **18**: 43. Doi: 10.1186/s12906-0182114z

Alyamani, A.A.; Albukhaty, S.; Aloufi, S.; AlMalki F.A.; Al-Karagoly, H.L. and **Sulaiman, G.M. (2021).** Green fabrication of zinc oxide nanoparticles using phlomis leaf extract: Characterization an vitro evaluation of cytotoxicity and antibacterial properties. *Molecules*, **26**(20): 6140. https://doi.org/10.3390/molecules 26206140

Arumugam, A.; Chandrasekaran, K.; Syedahamed, A.; Hameed, A.; Gopinath, K., Gowri, S.; Karthika, V. (2015). Synthesis of cerium oxide nanoparticles using *Gloriosa superba* L. leaf extract and their structural, optical and antibacterial properties**.** *Materials Science and Engineering*, **49**: 408-415.

Balogun, S.W.; Bello, S.A. and **Olayinka, O.H. (2021).** Influence of annealing temperature on the optical and structural properties of zinc oxide (ZnO) thin film as a transparent conductive oxide electrode. *Nano-plus. Sci. Tech. Nanomat*., **2**: 76-85.

Barzinjy, A.A. and **Azeez, H.H. (2020).** Green synthesis and characterization of zinc oxide nanoparticles using *Eucalyptus globulus* Labill leaf extract and zinc nitrate hexahydrate salt. *Springer Nature Journal*, **2**: 991. https://doi.org/10.1007/s42452-020-2813-1

Chenguo, H.; Zhang, Z.; Liu, H.; Gao, P. and **Wang, Z.L. (2006)**. Direct synthesis and structure characterization of ultrafine cerium oxide nanoparticles. *Nanotechnology*, **17**: 5983-5987.

CLSI (2012). Methods for dilution on antimicrobial susceptibility tests. 9th ed. 950 West Valley Road, Suite 2500, Wayne, Pennsylvania 19087, USA: *Clinical and Laboratory Standards Institute*, CLSI document M07eA9.

Diallo, A.; Ngom, B.; Part, E. and **Maaza, M. (2015).** Green synthesis of ZnO nanoparticles by *Aspalathus linearis*: structural and optical properties. *J. Alloys Compounds*, **646**: 425-430. Doi: 10.1016/j.jallcom.2015.05.242

Djearamane, S.; Sundaraji, A.; Eng, P.T.; Liang, S.X.T.; Wong, L.S. and **Senthilkumar, B. (2023).** Susceptibility of *Bacillus subtilis* to zinc oxide nanoparticles treatment. *Clin. Ter.*, **174**(1): 61-66. Doi: 10.7417/CT.2023.2498.

Elahi, B.; Mirzaee, M. and **Darroudi, M. (2018):** Preparation of cerium oxide nanoparticles in salvia *Macrosiphon boiss* seeds extract and investigation of their photo-catalytic activities. *Ceram. Int*., **45**(4): 4790–4797. Doi:10.1016/j.ceramint.11.173

Garani, S. and **Badsha, D.T. (2024)**. Impact of nanoparticles on haemato-physiological status of fish: A mini review. *Int. J. Pharm. Sci. Rev. Res*., **84**(3): 67-72. DOI: 10.47583/ijpsrr.2024.v84i03.010

Ghotekar, S. (2019). A review on plant extract mediated biogenic synthesis of CdO nanoparticles and their recent applications. *Asian J. Green Chem.,* **3**(2): 187–200.

Gnanasangeetha, D. and **Thambavani, S. D. (2014).** Facile and eco-friendly method for the synthesis of zinc oxide nanoparticles using *Azadirachta* and *Emblica*. *Int. J. Pharm. Sci. Res*., **5(7)**: 2866-2873.

Guzman, M.C.; Bistoni, M.A.; Tamagninii, L.M. and **Gonzalez, R.D. (2004):** Recovery of *Escherichia coli* in freshwater fish, *Jenynsia mulidenttata* and *Byrconamericus iheringi*. *Water Res*., **38**: 2368-2374.

Harekrishna, B.; Dipak, K.B.; Gobinda, P.S.; Priyanka, S.; Santanu, P. and **Ajay, M. (2009):** Green synthesis of silver nanoparticles using seed extract of *Jatropha curcas. Colloids* and *Surfaces A*: *Physicochemical* and *Engineering Aspects*, **348**: 212–216.

Harshitha, M.; Nayak, A.; Disha, S.; Satyaprasad, U.; Dubey, A.S.; Munang'andu, H.M.; Chakraborty, A.; Karunasagar, I. and **Biswajit, M. (2023).** Nanovaccines to combat *Aeromonas hydrophila* infections in warm-water aquaculture: Opportunities and challenges. Vaccines (Basel), **11**(10): 1555. Doi: 10.3390/vaccines11101555

He, L.; Su, Y. and **Lanhong, J. (2015):** Recent advances of cerium oxide nanoparticles in synthesis, Luminescence and biomedical studies: A review. *J. Rare Earths*, **33**(8): 791–799. Doi: 10.1016/S1002 0721(14)60486-5

Huang, O.; Yu, H. and **Ru, Q. (2009):** Bioavailability of and delivery of nutraceuticals using nanotechnology. *Food Science*, **75**: 50-56. Doi: 10.1111/j.1750-3841.01457.

Husain, K.W.; Patang, S. and **Rivai, A.A. (2023).** Effectiveness of papaya leaf extract (*Carica papaya* L.) for the treatment of koi (*Cyprinus rubrofuscus*) infected with *Aeromonas hydrophila* bacteria. *The international Journal of Science and Technology*, **11**(2): 7-13. https://doi.org/10.24940/theijst/2023/v11/i2/ST2302-003

Jan, H.; Shah, M.; Usman, H.; Khan, M.A.; Zia, M.; Hano, C. and **Abbasi, B.H. (2020)**. Biogenic synthesis and characterization of antimicrobial and antiparasitic zinc oxide (ZnO) nanoparticles using aqueous extracts of the Himalayan Columbine (*Aquilegia pubiflora*). *Front. Mater.* **7**: 249. Doi: 10.3389/fmats.2020.00249

Jin, S.E. and **Jin, H.E. (2021).** Antimicrobial activity of zinc oxide nano/microparticles and their combinations against pathogenic microorganisms for biomedical applications: From physicochemical characteristics to pharmacological aspect. *Nanomaterials (Basel)*, **11**(2): 263. Doi: 10.3390/nano11020263

Kumar, A.; Das, S.; Munusamy, P.; Self, W.; Baer, D.R.; Sayle, D.C. and **Seal, S. (2014):** Behaviour of nanoceria in biologically-relevant environments. *Environ. Sci. Nano*, **1**: 516–532.

Kwabena, D.E. and **Aquisman, A.E. (2019):** Morphology of green synthesized ZnO nanoparticles using low temperature hydrothermal technique from aqueous *Carica papaya* extract. *Nanoscience and Nanotechnology*, **9**(1): 29-36. Doi:10.5923/j.nn.20190901.03. ISSN: 2163-257X e-ISSN: 2163-2588

Maqbool, Q.; Nazar, M. and **Naz, S. (2016):** Antimicrobial potential of green synthesized CeO2 nanoparticles from *Olea europaea* leaf extract. *Int. J. Nanomedicine*., **11**: 5015–5025. doi:10.2147/IJN.S113508

Miri, A.; Darroudi, M. and **Sarani, M. (2019):** Biosynthesis of cerium oxide nanoparticles and its cytotoxicity survey against colon cancer cell line. *Appl. Organomet. Chem*., **34**(1): 1-15.

Muahiddah, N. and **Diamahesa, W.A. (2023).** The use of immunostimulants from papaya leaves to treat disease and increase non-specific immunity in fish and shrimp. *Journal of Fish Health*, **3**(1): 19-24. https://doi.org/10.29303/jfh.v3i1.2755

Nagarathna, S.B.; Jain, S.K.; Arun, H.R.; Champawat, P.S.; Mogra, R. and **Maherchandani, J.K. (2021).** An overview of papaya: Phytochemical constituents and its therapeutic publications. *The Pharma Innovation Journal*, **10**(9): 45-49.

Natarajan, S. and **Vidhya, R.M. (2014):** Potential medicinal properties of *Carica papaya* Linn: A mini review. *Int. J. Pharm. Sci.*, **6**: 1-4.

Nateghi, M.R. and **Hajimirzababa, H. (2014):** Effect of silver nanoparticles morphologies on antimicrobial properties of cotton fabrics. *J. Text. Inst*., **108**: 806–813.

Nikalje, A.P. (2015): Nanotechnology and its application in medicine. *Medicinal chemistry*, **5**: 081-089. Doi10.4172/2161-0444.1000247

Noorjahan, C.M. (2019): Green synthesis, characterization, and antibacterial activity of zinc oxide nanoparticle. *Asian journal of pharmaceutical and clinical research*, **12(**4): 106-110.

Parashar, U.K. and **Srivastava, S.P. (2009).** Bioinspired synthesis of silver nanoparticles. *Digest Journal of Nanomaterials and Biostructures*, **4** (1): 159-166.

Paul, B.I.; Nasreen, M.A.; Sarker, A.N. and **Islam, M.R. (2013):** Isolation, purification and modification of papain enzyme to ascertain industrially valuable nature. *Int. J. Biotechnol*. Res., **3**(5): 11–22.

Pelgrift, R. and **Friedman, A. (2013):** Nanotechnology and a therapeutic tool to combat microbial resistant: A review. Journal of advance drug delivery, **65**: 13-14. PubMed DOI:10.1016/j.addr.2013.07.011

Rahmani, A.H. and **Aldebasi, Y.H. (2016).** Potential role of *Carica papaya* and their active constituents in the prevention and treatment of diseases. *Int. J. Pharm. Pharm. Sci*., **8**(1): 11–15.

Rani, J.S. (2020): Green synthesis and characterization of ceria Nps (Cerium oxide nanoparticles) using *Ricinus Communis* leaf extract. *International Journal of Scientific and Research Publication*, **10**(1): 286-291.

Renganathan, S.; Aroulmoji, V.; Shanmugam, G.; Devarajan, G.; Rao, K.V.; Rajendar, V. and **Park, S. (2018):** Silver nanoparticle synthesis from *Carica papaya* and virtual screening for anti-dengue activity using molecular docking. Mater. Res. Express, 6(3): 5028. *https://doi.org/10.1088/2053- 1591/aaf6f* 6 035028

Robinson, I.; Zacchini, S.; Tung, L.D.; Maenosono, S. and **Thanh, N.T.K. (2009).** Synthesis and characterization of magnetic nanoalloys from bimetallic carbonyl clusters. *Chemistry of Materials*, **21**(13): 3021–3026. Doi: 10.1021/cm9008442.

Sarkar, D.J.; Mohanty, D.; Raut, S.S. and **Das, B.K. (2022).** Antibacterial properties and in silico modelling perspective of nano ZnO transported oxytetracycline-Zn^{2+} complex $[ZnOTc]^{+}$ against oxytetracycline-resistant *Aeromonas hydrophila. The Journal of Antibiotics*, **75**: 635–649.

Shaalan, M.; Saleh, M.; El-Mahdy, M. and **El-Matbouli, M. (2016).** Recent progress in applications of nanoparticles in fish medicine: A review. *Nanomed. Nanotechnol. Biol. Med.*, **12**: 701–710. Doi: 10.1016/j.nano.2015.11.005.

Sharma, V.K.; Yngard, R.A. and **Lin, Y. (2009):** Silver nanoparticles: Green synthesis and their antimicrobial activities. Advances in Colloid and Interface Sci., **145**: 83-96.

Shen, Z.C.; Zhou, H.J.; Chen, H.Y.; Xu, H.; Feng, C.H. and **Zhou, X.H. (2018).** Synthesis of nano-zinc oxide loaded on mesoporous silica by coordination effect and its photocatalytic degradation property of methyl orange. *Nanomaterlals*-Basel., **8(5)**: 317.

Sherif, A.H.; Abdelsalam, M.; Ali, N.G. and **Mahrous, K.F. (2023).** Zinc Oxide nanoparticles boost in *Oreochromis niloticus* and improve disease resistance to *Aeromonas hydrophila* infection. Biol. Trace. Elem. Res., **201**(2): 927-936. Doi: 10.1007/s12011-022-03183-w.

Singh, S.P.; Kumar, S.; Mathan, S.V.; Tomar, M.S.; Singh, R.K.; Verma, P.K.; Kumar, A.; Sandeep K.; Singh, R.P. and **Arbind Acharya, A. (2020):** Therapeutic application of *Carica papaya* leaf extract in the management of human diseases. *Journal of Pharmaceutical Sciences*. Springer Nature Switzerland, **28**: 735–744. https://doi.org/10.1007/s40199-020-00348-7

Singh, S.P.; Kumar, S.;Tomar, M.S.; Singh, R.K.; Verma, P.K. and **Kumar, A. (2019):** Aqueous extract of *Carica papaya* leaf elicits the production of TNF-α and modulates the expression of cell surface receptors in tumor-associated macrophages. *Biosc. Biotech. Res*., **4**: 1115–1122.

Timkur, P.P.; Gunasekaran, N.K.; Lamani, B.R.; Bayon, N.N.; Prabhakaran, K.; Hall, J.C. and **Ramash, G.T. (2021):** Cerium oxide nanoparticles: Synthesis and characterization for biosafe applications. *Nanotechnology*, **1**(3): 176-189.

Upadhyaya, H.; Shome, S.; Sarma, R.; Tewari, S.; Bhattacharya, M. and **Panda, S. (2018).** Green synthesis, characterization and antibacterial activity of ZnO nanoparticles. *American Journal of Plant Sciences*, **9**: 1279-1291. Doi: 10.4236/ajps.2018.96094

Yass, M.; Al-Haddad, A.; Ali, M. J.; Jaafar, A. and Veres, M. (2023). Effectiveness of Green Synthesized Zinc Oxide Nanoparticles against Extensively Drug resistant *Klebsiella Pneumonia. Biomedical and Biotechnology Research Journal* 7(3): 497-503, DOI: 10.4103/bbrj.bbrj_167_23